Published version available at: https://doi.org/10.1080/13647830.2022.2121663

Lifted jet edge flames: symmetric and non-symmetric configurations

Vadim N. Kurdyumov [1], **Carmen Jiménez**

Department of Energy, CIEMAT, Avda. Complutense 40, 28040 Madrid, Spain

Abstract

The purpose of this work is to demonstrate that there are different stable configurations of lifted edge flames for the same set of parameters. It is shown that when a fuel jet is injected surrounded by oxidizer streams of equal velocity, there are configurations with symmetric and non-symmetric flame structures with respect to the symmetry line of the problem. These two kinds of solutions are both stable and the actual realization of one or another solution depends on the initial conditions, in particular on the flame ignition parameters. It is shown that this multiple solution phenomenon takes place when the fuel Lewis number is less than unity. The influence of the Zel'dovich number and the injection flow rate is also investigated.

1 Introduction

One of the possible advantages of using diffusion flames in combustion devices is the greater safety of the system operation. Indeed, when the fuel and oxidant are fed into the combustion zone through different channels, without prior mixing, the possibility of appearance of dangerous phenomena such as the flash-back effect, for example, when the flame propagates upstream out of control, is significantly reduced.

Perhaps the most investigated topic related to laminar diffusion flames in recent decades has been the study of edge flames carried out within different models, where the structure, the dynamics and the influence on them of effects such as heat losses or thermal expansion were under consideration. One needs to separate two large segments of these investigations. The first one focuses on edge flames moving along the mixing layer; and in these studies the propagation speed itself is to be found as part of the solution, see [1–8].

Another group of studies is mainly concerned with the structure and dynamics of the edge flame situated near the tip of the plate which separates the fuel and oxidizer upstream [9–17]. The edge-flame behavior in the corner region of their two mutually perpendicular streams of

[1]Corresponding author

fuel and oxidizer has also been investigated in [18]. In these cases, the problem does not include the determination of the edge-flame propagation speed (the problem eigenvalue). Important references to other earlier works can be found in [19, 20]. A recent review of issues related to diffusion flames involving edge-flames with a focus on the effect of hydrodynamics is presented in [21].

The relatively frequent phenomenon of multiplicity of steady state solutions has been demonstrated in some recent studies on the structure of laminar flames. This phenomenon occurs, for example, when a premixed flame propagates in a narrow channel, where it has been shown that symmetric and non-symmetric flames with respect to the middle of the channel may appear, see e.g. [22–24]. This effect is related to the strong nonlinearity of the equations.

It should be noted that very frequently one type of solution is stable while the other one is not. However, a different situation, where several steady-state solutions are stable simultaneously, is also possible. When this is the case, then the realization of one or another final solution depends on the initial conditions. The purpose of this work is to show that for flames of the diffusion type, namely without preliminary mixing of the fuel and oxidizer, a similar situation is possible with multiple stable steady-state solutions.

Studies of flame behavior and their interpretation are complicated by the fact that several physical phenomena manifest themselves simultaneously. Among the most important ones, we can distinguish the fluid-flame interaction due to thermal expansion, the flame-wall heat exchange and the differential diffusion effect. Nevertheless, even a model which includes only these three phenomena remains sufficiently complicated in order to get a clear physical insight with an unambiguous explanation of the appearance of a particular flame behavior.

One of the possible approaches to this question is to use successively simplified models, in which some of the above effects are excluded from consideration. These simplifications may bring the quantitative results away from reality, but in compensation they provide a clearer understanding of the true cause of the effect under study. On the other hand, if an effect exists within a simple model, we can be confident that it should persist under more realistic assumptions.

The present work investigates the structure of the pair of edge flames that can be formed as a planar fuel jet emerges into a co-flowing oxidizer jet at the same speed. The study is carried out on the basis of a thermo-diffusive model used in many theoretical and numerical investigations [2, 4, 5, 7, 9–11, 13, 16, 18]. The article is structured as follows. The next section presents the mathematical formulation of the problem. The solution method is briefly described

in Section 3. The results of the numerical analysis are presented in Section 4 . The last Section provides conclusions.

2 Formulation

Let us consider two semi-infinite parallel plates, as shown in Fig. 1, separating streams of equal velocity U_0, one of fuel with mass fraction Y_{F0} flowing between the plates, and the others of oxidizer with mass fraction Y_{O0}, emanating on both sides of the central fuel stream. The distance between the plates is h. It is assumed that the thermal conductivity of the plates is sufficiently high so as to maintain their temperature constant and equal to the upstream temperature T_0. After the ends of the plates fuel and oxidizer interdiffuse, thereby generating initially two parallel mixing layers thickening downstream. In the absence of burning, the two mixing layers merge at some distance. This is illustrated in Fig. 1, where the isolines of fuel mass fraction are shown at interval 0.1.

When ignition is successful, a gas-phase oxidation chemical reaction takes place within the mixing layers. In each mixing layer the flame consists of the well-known edge flame located at a distance from the tip of the plate accompanied by a diffusion flame that separates the fuel and oxidizer. Since the total fuel flux is finite, these two diffusion flames have a finite length downstream, merging with each other. Perhaps, this configuration is the simplest one in which lifted flames can be considered.

The chemical reaction is modeled by an overall irreversible one step of the form

$$\mathrm{Fuel} + \nu\,\mathrm{Oxidizer} \rightarrow (1+\nu)\mathrm{Product},$$

where ν is the mass-weighted stoichiometric coefficient. The fuel consumption rate per unit volume is assumed to be first order with respect to each of the two reactants and obeys an Arrhenius law, $\Omega = \mathcal{B}\rho^2 Y_F Y_O \exp(-\mathcal{E}/\mathcal{R}T)$, with a preexponential factor $\mathcal{B}$ and an overall activation energy $\mathcal{E}$. Here Y_F and Y_O are the mass fractions of fuel and oxidizer, respectively, T and ρ are the temperature and density of the mixture, and $\mathcal{R}$ is the universal gas constant.

We consider a diffusive-thermal model, according to which the density of the mixture ρ, the thermal diffusivity $\mathcal{D}_T$, the heat capacity c_p, and the individual molecular diffusivities $\mathcal{D}_F$ and $\mathcal{D}_O$ of fuel and oxidizer are all assumed constant. Under this assumption, the problem is governed by the balance equations for the mass fraction of each of the two species and an energy equation for the whole mixture.

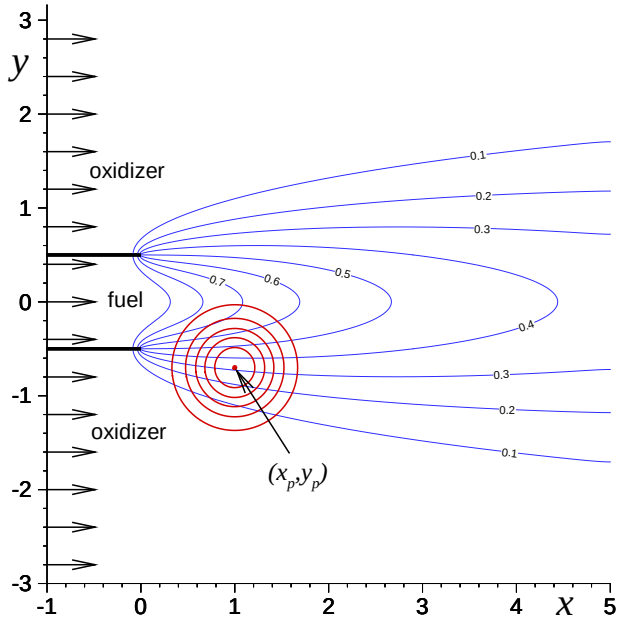

Figure 1: Sketch of the problem, coordinate system, initial distribution of the normalized fuel mass fraction (isolines at interval 0.1) and initial hot spot for the temperature field given by Eq. (8) (circles, isolines at interval 0.1).

The mass fractions are normalized with respect to their values in the supply streams Y_{F0} and Y_{O0}, respectively, and a nondimensional temperature $\theta = (T - T_0)/(T_a - T_0)$ is introduced, where $T_a = T_0 + QY_{F0}/c_p(1 + \phi)$ is the adiabatic flame temperature (of the corresponding stoichiometric fuel-oxidizer mixture). Here Q is the total heat release per unit mass of fuel and $\phi = \nu Y_{F0}/Y_{O0}$ the mixture equivalence ratio. Using h as unit of length and h/U_0 as unit of time, the dimensionless governing equations take the form

$$m\left(\frac{\partial\theta}{\partial t} + \frac{\partial\theta}{\partial x}\right) = \nabla^2\theta + (1+\phi)\omega \tag{1}$$

$$m\left(\frac{\partial Y_F}{\partial t} + \frac{\partial Y_F}{\partial x}\right) = Le_F^{-1}\nabla^2 Y_F - \omega \tag{2}$$

$$m\left(\frac{\partial Y_O}{\partial t} + \frac{\partial Y_O}{\partial x}\right) = Le_O^{-1}\nabla^2 Y_O - \phi\omega \tag{3}$$

with the dimensionless reaction rate ω given by

$$\omega = D\beta^3 Y_F Y_O \exp\left(\frac{\beta(\theta-1)}{(1+q\theta)/(1+q))}\right) \tag{4}$$

The parameters appearing in the above equations are the dimensionless flow velocity $m = hU_0/\mathcal{D}_T$ (called also the Peclet number), the Lewis numbers associated with the fuel and oxidizer $Le_F = \mathcal{D}_T/\mathcal{D}_F$ and $Le_O = \mathcal{D}_T/\mathcal{D}_O$, respectively, the heat release parameter $q = (T_a - T_0)/T_0$, the Zeldovich number $\beta = \mathcal{E}(T_a - T_0)/RT_a^2$, and the Damköhler number $D = (h^2/\mathcal{D}_T)\rho\mathcal{B}Y_{O0}\beta^{-3}\exp(-\mathcal{E}/\mathcal{R}T_a)$. All calculations below were carried out for $\phi = 1$ and $q = 5$.

The boundary conditions for the problem can be written as follows:

$$y = \pm 1/2,\, x < 0: \quad \theta = \partial Y_F/\partial y = \partial Y_O/\partial y = 0 \tag{5}$$

$$x \to -\infty: \quad \theta = 0, \quad \begin{cases} Y_F = 1, \quad Y_0 = 0 & \text{for} \quad -1/2 < y < 1/2, \\ Y_F = 0, \quad Y_0 = 1 & \text{for} \quad y < -1/2 \quad \text{and} \quad y > 1/2, \end{cases} \tag{6}$$

and

$$x \to \infty: \quad \partial^2\theta/\partial y^2 = \partial^2 Y_F/\partial y^2 = \partial^2 Y_O/\partial y^2 = 0, \tag{7}$$

where more relaxed conditions for variables than zero first derivatives are used.

To start the calculations, the frozen distributions for Y_F and Y_O calculated by imposing $\omega \equiv 0$ in Eq. (2)-(3) were used. The initial temperature field was chosen in the form of a hot spot given by

$$t = 0: \quad \theta = \theta_{max}\exp(-[(x-x_p)^2 + (y-y_p)^2]/a^2)\,, \tag{8}$$

where θ_{max} is the maximum initial temperature value, (x_p, y_p) is its location, and a is the characteristic radius of the initial hot spot. For $y_p = 0$, the initial temperature field is symmetrical with respect to the middle of the channel $y = 0$.

In the calculations presented below the heat release coefficient was assigned the fixed value $q = 5$ and, unless otherwise specified, the Zeldovich number was fixed at $\beta = 10$. The mixture equivalence ratio was chosen as $\phi = 1$. For the numerical parameters of the initial temperature distribution determined by Eq. (8) $\theta_{max} = 0.6$, $x_p = 1$ and $a = 0.5$ were chosen, while the value of y_p was varied in the calculations. An example of the initial temperature field is illustrated in Fig. 1.

In order to characterize the flame structure quantitatively, a symmetry index was calculated

$$S = \int_{x_{min}}^{x_{max}} dx \int_0^{y_{max}} y \cdot [\theta(x,y,t) - \theta(x,-y,t)]dy\,. \tag{9}$$

When calculated in a domain of finite size, the numerical value of S depends on the size of the computational domain. The symmetry index S has no special physical meaning, it is just a measure of the flame symmetry. Obviously, if the solution is symmetric with respect to the line $y = 0$, then $S = 0$ (within the calculation accuracy). The y factor is included in Eq. (9) only to distinguish the values of S for hot spots with the same width a but different transverse position y_p.

Speaking in a strict mathematical sense, $S = 0$ can be obtained also occasionally for a non-symmetric distribution of a special kind. However, the most important feature is that having a non-zero value of S, one can be sure that the temperature distribution is not symmetric. In any case, the information obtained from the value of S was verified by direct visual observation of the temperature field and $S = 0$ values for non-symmetrical distributions were never obtained for all the cases considered.

Another convenient characteristic used below to identify the flame structure is the edge flame position. This value is determined by the point (x_w, y_w) where the reaction rate achieves its local maximum value, $\omega_{max} = \omega(x_w, y_w)$. In the considered burner configuration there are two edge flames located behind each plate separating the flows of fuel and oxidizer, one in the lower half-plane, (x_{w1}, y_{w1}) with $y_{w1} < 0$, and the other in the upper half-plane, (x_{w2}, y_{w2}) with $y_{w2} > 0$. Obviously, for a symmetrical flame structure we have $x_{w1} = x_{w2}$ and $y_{w1} = -y_{w2}$.

3 Numerical treatment

All calculations were carried out in a finite domain, $x_{min} < x < x_{max}$ and $y_{min} < y < y_{max}$. The transverse size of the domain was chosen so as to have zero temperature at the maximum and minimum values in y. Typical values were $x_{min} = -1$, $x_{max} = 5$ and $y_{max} = -y_{min} = 3$.

Two numerical methods were applied. The first is a direct time-marching method. Eqs. (1)-(3) were discretized using finite difference second-order, three-point approximation for space derivatives and first-order discretization in time. The presence of the highly nonlinear reaction rate term requires indirectly to choose the time step sufficiently small so as to ensure numerical stability.

The time-dependent calculations were tested on three different grids, namely grids with 301×301, 481×481 and 601×601 points. To start the calculations, the value of the time step was $\tau = 10^{-5}$. After the calculations were advanced up to $t = 2$, the value of τ was increased up to 10^{-4}.

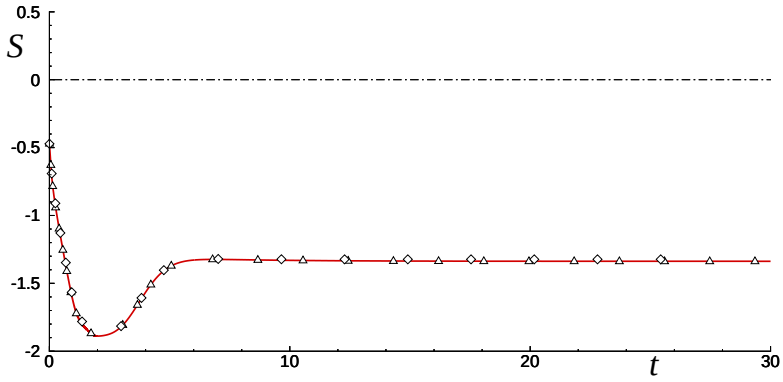

Figure 2: An example of comparing the results for the symmetry index time evolution calculated on different grids: 301×301 (circles), 481×481 (solid line) and 601×601 (triangles).

Figure 2 illustrates the time dependence for S obtained on different grids. The solid curve shows the result obtained on the 481×481 grid, while the open circles and triangles are obtained on the smaller and coarser grids. It can be seen that the results differ very little. Thereafter, most of the calculations were made on the intermediate grid.

To obtain steady-state solutions (possibly unstable in some cases), $\partial/\partial t \equiv 0$ were applied in Eq. (1)-(3) and the Gauss-Seidel iteration method was executed. In this case, the temperature value at some point was fixed while the flow velocity was calculated iteratively. The details of this procedure were described in detail in [10].

4 Results

4.1 Time-dependent calculations

Figures 3 and 4 show sequences of snapshots which illustrate the flame evolution after placing a hot spot until a steady-state solution is established. All plots represent the temperature field using the same color legend. Parameter values are fixed at $m = 14$, $Le_F = 0.7$, $Le_O = 1$, $D = 400$, $\beta = 10$ and $q = 5$. The only difference for the two illustrated cases (Fig. 3 and Fig.4) is the position of the initial hot spot. For Fig. 3 we used $(x_p, y_p) = (1, -1)$ while for Fig. 4 the location is $(x_p, y_p) = (1, -0.4)$. It can be seen that the difference in the vertical location of the hot spot y_p results in two different final flame configurations, one symmetric and one non-

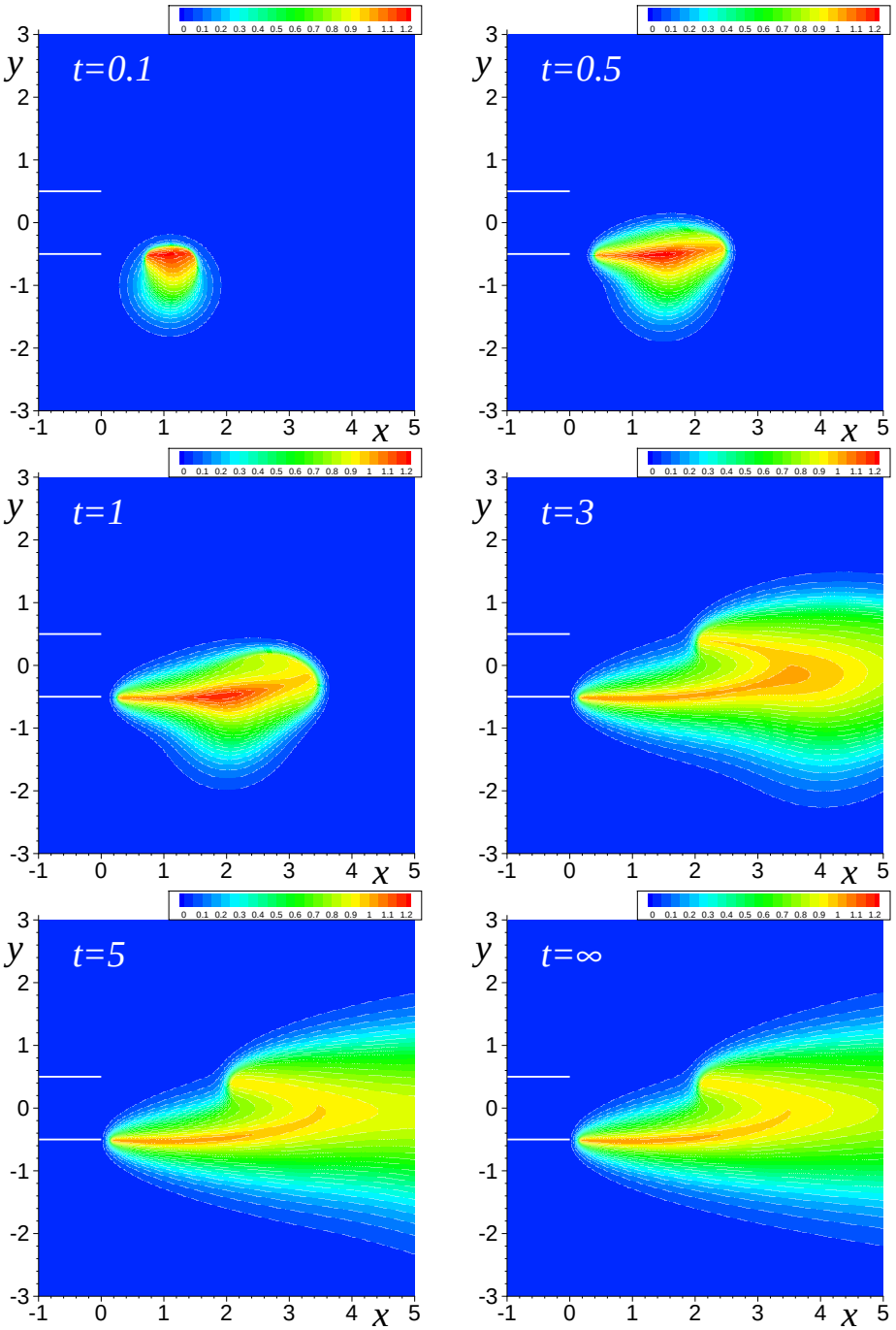

Figure 3: The sequence of snapshots of the temperature field obtained with the location of the initial hot spot at $(x_p, y_p) = (1. - 1)$ calculated for $m = 14$, $Le_F = 0.7$, $Le_O = 1$ and $\beta = 10$ illustrating the formation of a non-symmetric state of the edge-flames.

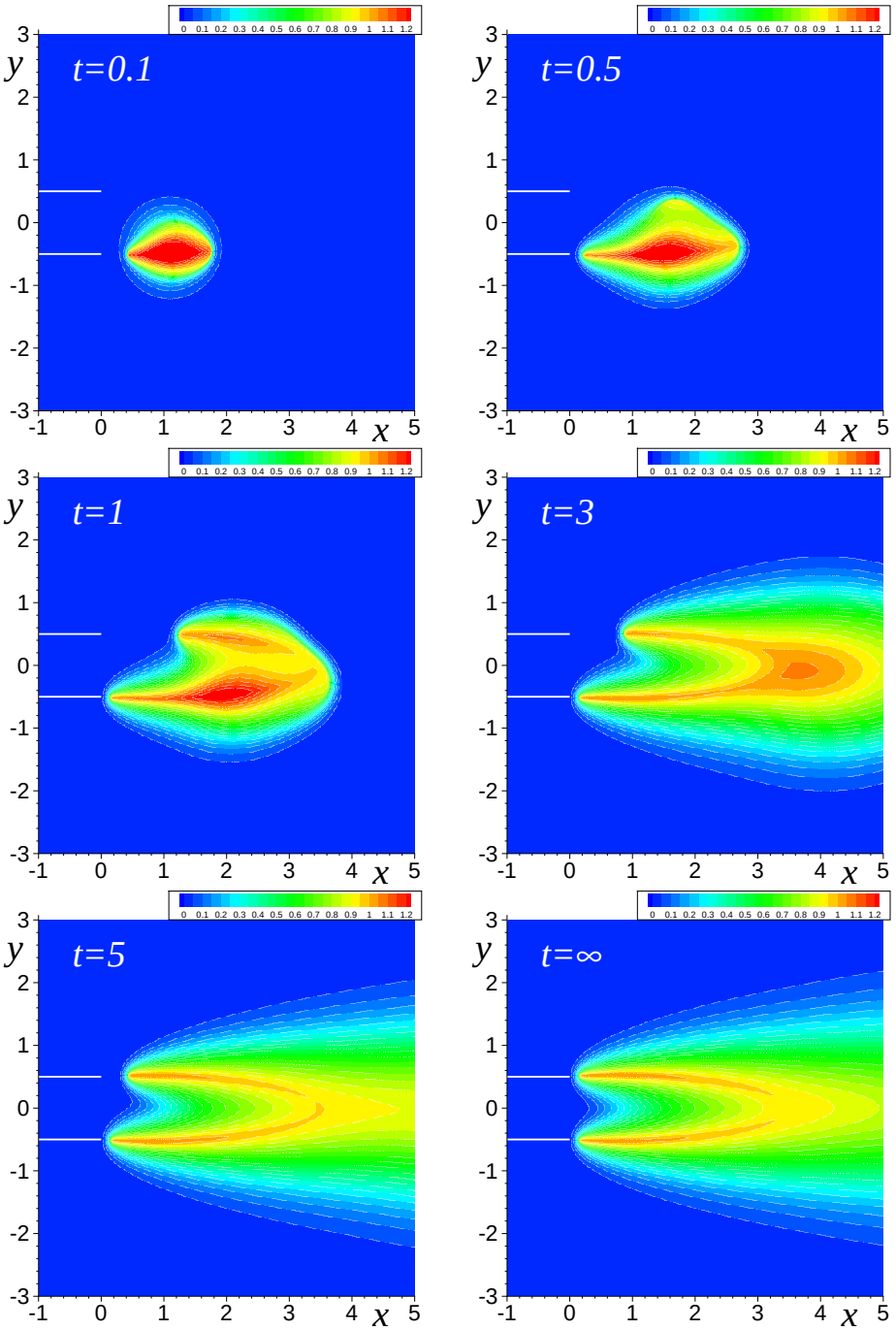

Figure 4: The sequence of snapshots of the temperature field obtained with the location of the initial hot spot at $(x_p, y_p) = (1. - 0.4)$ calculated for $m = 14$, $Le_F = 0.7$, $Le_O = 1$ and $\beta = 10$ illustrating the formation of a symmetric state of the edge-flames.

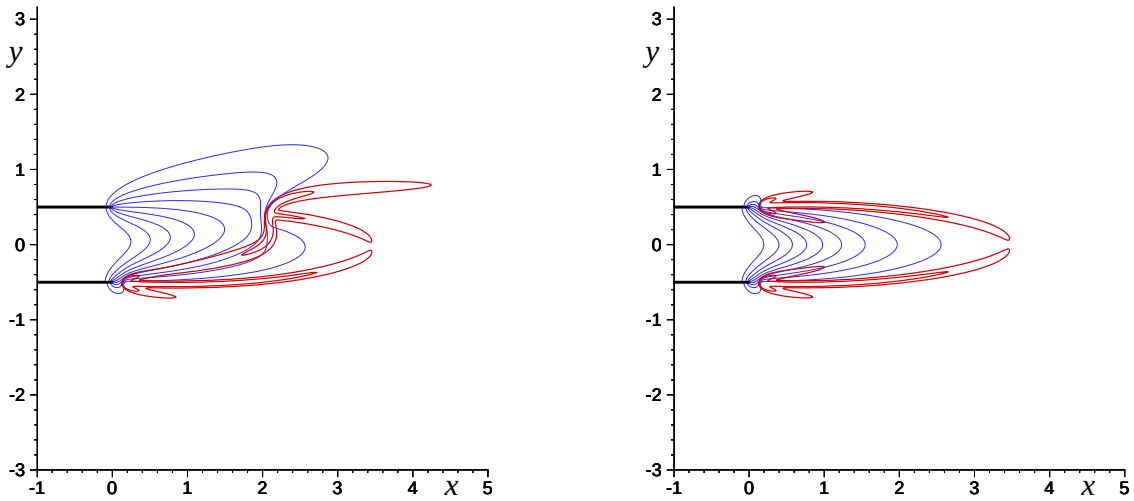

Figure 5: The final distributions of the reaction rate (isolines $\omega = 1$ and 10) and the fuel mass fraction (with a step of 0.1) for the non-symmetric and symmetric states.

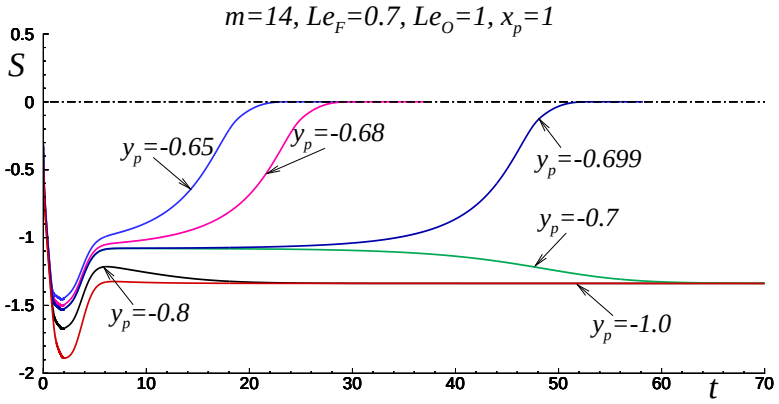

Figure 6: Time evolution of the symmetry index S for $Le_F = 0.7$ and $Le_O = 1$ and various initial hot spot positions y_p; $x_p = 1$ for all curves.

symmetric. Figure 5 shows the distributions of the reaction rate (isolines with $\omega = 1$ and 10) along with the fuel mass fraction distribution (with 0.1 spacing) for the final symmetrical and non-symmetrical solutions.

The presented numerical simulations reveal that the structure of the final state, symmetrical

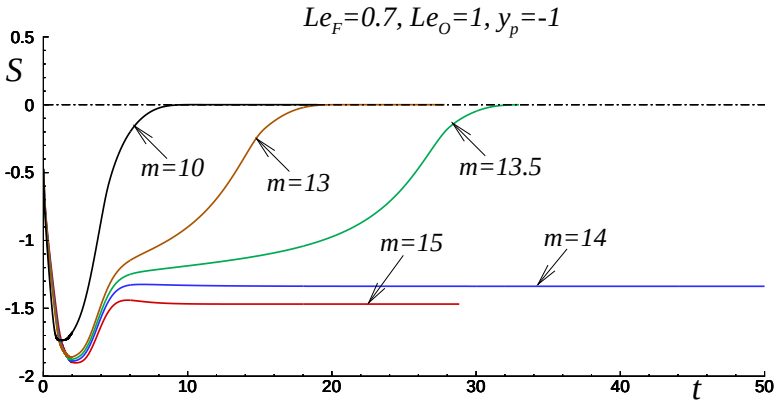

Figure 7: Time evolution of the symmetry index S for $Le_F = 0.7$ and $Le_O = 1$ for different flow rates m with the same localization of the initial hot spot at $(x_p, y_p) = (1, -1)$.

or non-symmetrical, depends on the initial location of the hot spot used for ignition. When it is located at a sufficient distance from the line of symmetry $y = 0$, then a state with a non-symmetrical arrangement of edge-flames is established. The dependencies of the symmetry index on time for different y_p are shown in Fig. 6 illustrating this result. The value of the x-location is chosen at $x_p = 1$ for all curves shown in the figure. Of course, the critical value for the hot spot transverse coordinate also depends on its longitudinal position and has no universal meaning in and of itself.

Figure 7 shows the temporal dynamics of the symmetry index when the hot spot is located at $(x_p, y_p) = (1, -1)$ calculated for various values of the dimensionless gas velocity m. It can be seen that for the formation of a non-symmetric final state, the gas velocity should also exceed a certain critical value. At velocities below the critical velocity, a symmetrical edge-flame state occurs (for the same initial hot spot location).

All the results presented so far have been calculated with $Le_O = 1$ and $Le_F = 0.7$. Figure 8 shows the dynamics of the symmetry index obtained with $Le_O = Le_F = 1$ for various values of m. One can see that all final states have $S = 0$. In all likelihood, the effect of non-symmetric flame structure is associated with the choice of the fuel Lewis number less than unity. Of course, a finite set of numerical calculations can not guarantee that a non-symmetrical structure could not appear for other values of the parameters. However, it can be seen that for $Le_F = Le_O = 1$, non-symmetric flames were not observed for the considered cases.

Figure 9 shows the time dependence of the symmetry index S calculated for the same loca-

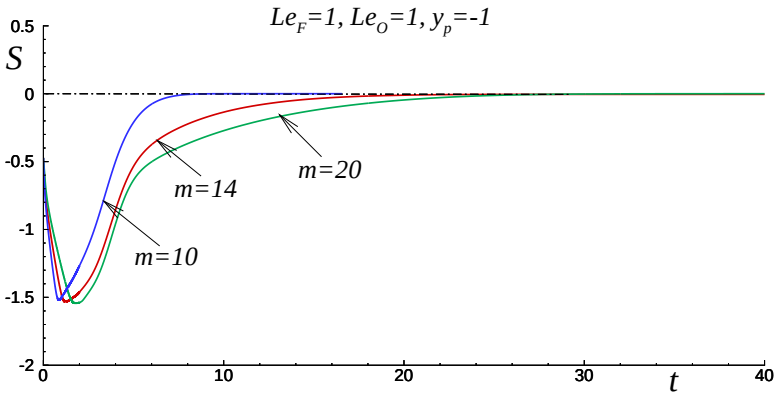

Figure 8: Time evolution of the symmetry index S for $Le_O = Le_F = 1$ and various flow rates m; all cases are calculated with $(x_p, y_p) = (1, -1)$.

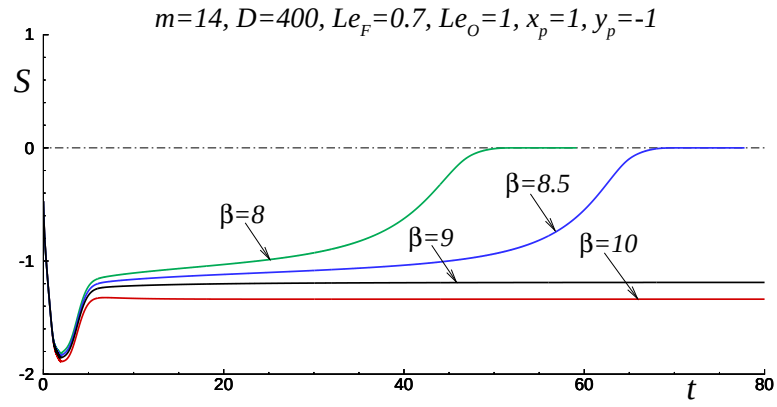

Figure 9: Time evolution of the symmetry index S for $Le_O = 1$, $Le_F = 0.7$ and various β; all curves are calculated for $(x_p, y_p) = (1, -1)$.

tion of the initial hot spot for flames with different values of the Zel'dovich number β. The rest of the parameters are also chosen to be the same as in previous calculations. The dependence shown in Fig. 9 suggests that for the formation of an non-symmetric combustion structure, the Zel'dovich number must exceed a certain critical value (between 8 and 9). Considering that $\beta \sim (T_a - T_0)/T_a^2$, it can be concluded that a non-symmetrical flame structure is more likely to be seen for cases with lower adiabatic temperature, in other words, for weaker flames.

All previous results were obtained for $D = 400$. The influence of the Damköhler number on the stabilization of non-symmetric combustion patterns was also investigated. Figure 10 shows

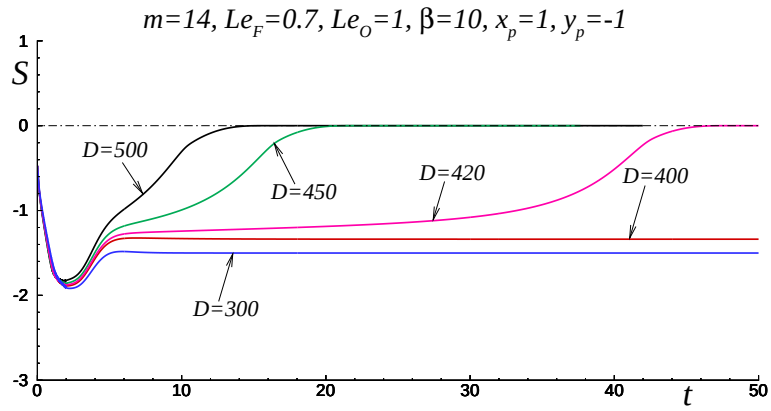

Figure 10: Time evolution of the symmetry index S for $Le_O = 1$, $Le_F = 0.7$, $\beta = 10$ and various reduced Damköhler number D; all curves are calculated for $(x_p, y_p) = (1, -1)$.

the evolution of the symmetry index over time for different values of D. All curves correspond to a hot spot located at $(x_p, y_p) = (1, -1)$ and $m = 14$, $\beta = 10$. It can be seen that when the Damköhler number increases above a certain critical value, with other parameters fixed, the formation of an non-symmetric combustion pattern does not occur and the final state turns out to be symmetrical.

Intuitively, we can imagine that when a sufficiently intense perturbation is added to a non-symmetric configuration, for example in the form of a hot spot located on the opposite side (at $y > 0$), the edge flame configuration recovers a symmetrical state. This is illustrated in Fig. 11, where a sequence of the temperature field (color plots) and the reaction rate isolines (levels at 1 and 10) shows the development of the flame structure. The calculated non-symmetric state was taken as initial condition with a hot spot added in the upper half in the form $\delta\theta = \delta\theta_* \exp(-[(x - x_*)^2 + (y - y_*)]/a_*^2)$. The numerical values of the hot spot parameters used to plot Fig. 11 were $\delta\theta_* = 0.4$, $x_* = 1$, $a_* = 0.5$ and $y_* = 0.5$. The initial non-symmetric solution became rapidly symmetric, as shown in the sequence.

It should be noted that in order to force the transition from a non-symmetric to a symmetric states, the temperature of the hot spot must exceed a certain threshold value. Figure 12 shows the evolution of the symmetry index for different values of $\delta\theta_*$. In this figure, the dashed line corresponds to the value $S \approx -1.33871$ calculated for the steady-state non-symmetric case. At the beginning of the calculations, the value of S slightly exceeds this value due to the hot spot added to the non-symmetrical temperature distribution. It can be seen that for sufficiently

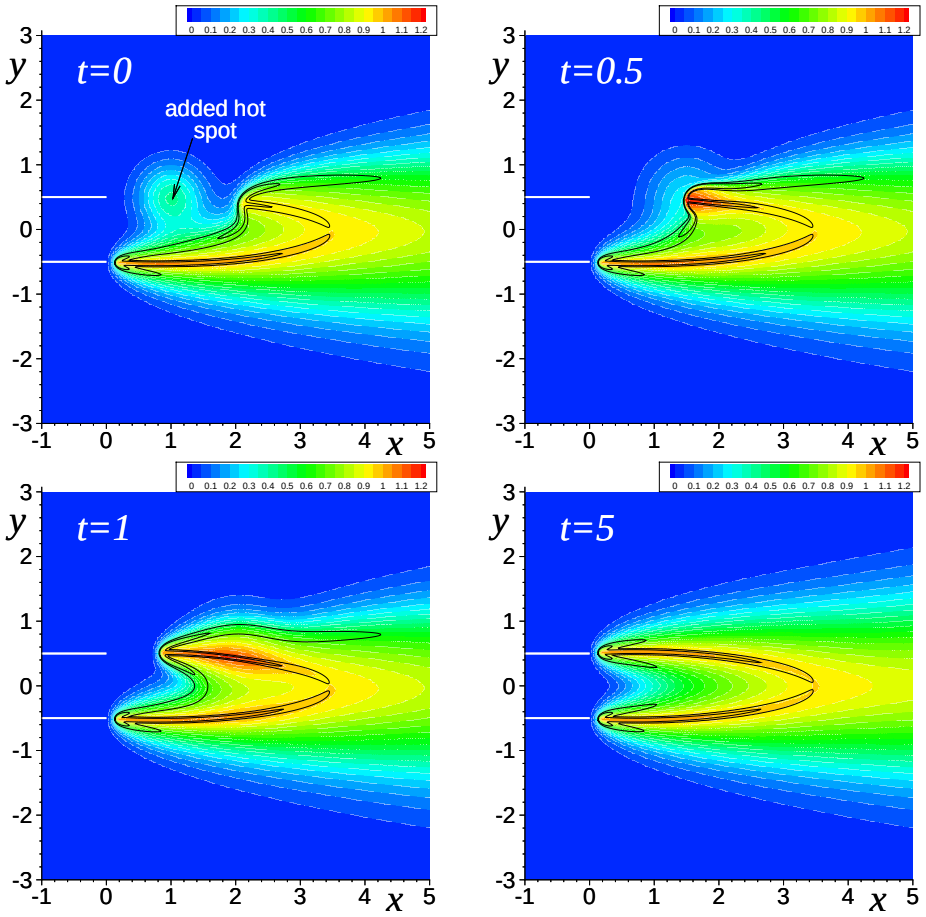

Figure 11: The sequence of snapshots of the temperature field (color plot) and the reaction rate isolines ($\omega = 1$ and 10) obtained from the non-symmetric edge flame configuration with an added hot spot located in at $(x_*, y_*) = (1., 0.5)$; for calculated for $m = 14$, $Le_F = 0.7$, $Le_O = 1$ and $\beta = 10$ illustrating transition from non-symmetric to symmetric configurations.

large perturbations, the system evolves into a symmetrical state. However, for sufficiently small perturbations (e.g. the curves with $\delta\theta_* = 0.02$ and 0.05) the system returns to a non-symmetric state. This result once again confirms that the non-symmetric state is stable for (sufficiently) small perturbations.

4.2 Steady-state results

It is well known that an edge-flame situated behind the tip of a cold isothermal plate separating the streams of fuel and oxidizer can exist only within a certain range of the flow rate, $m_{min} <$

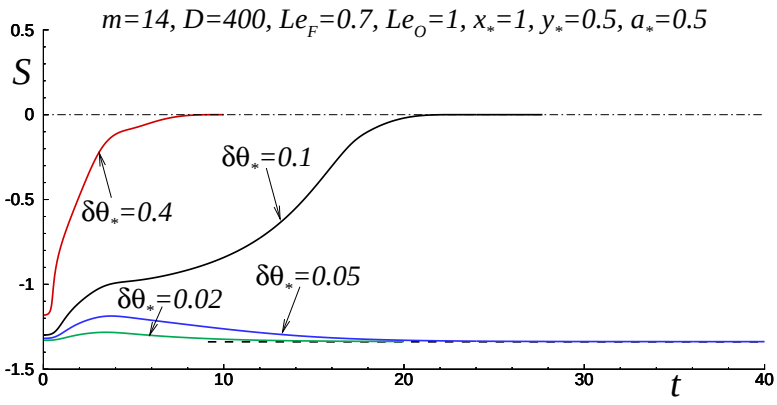

Figure 12: Time evolution of the symmetry index S for $Le_O = 1$, $Le_F = 0.7$, $\beta = 10$ and different hot spot intensity values. The dashed line shows the S value for the non-symmetrical solution.

$m < m_{max}$ [9–11]. When the flow rate decreases, $m \to m_{min}$, the heat loss from the flame to the plate increases causing the flame extinction. With an increase in the flow rate, $m \to m_{max}$, the edge flame moves away from the tip of the plate and is eventually blown-off. It is also well known that the distance between the edge-flame and the tip of the plate reaches a minimum value at intermediate values of the flow rate.

Numerical results regarding symmetric and non-symmetric steady states are summarized in Fig. 13 for $Le_F = 0.7$, $Le_O = 1$, $D = 400$ and $\beta = 10$. The left plot shows the x-position of the edge flame and the right plot displays the values of the symmetry index as functions of the flow rate. Dependencies corresponding to a symmetrical flame, x_w and S, are shown by dashed lines. The positions of the edge flames in the lower, x_{w1}, and upper, x_{w2}, half-spaces for non-symmetrical configurations are drawn with solid lines. Taking into account that there are two configurations mirrored with respect to $y = 0$ for any non-symmetrical flame, the right plot shows both the negative and positive branches of S. Fig. 13 shows that although the maximum values for the flow rate in the cases of symmetrical and non-symmetrical flames are close to each other, the minimum values differ significantly. Critical points are marked on the figure by open circles.

The closeness of the maximum critical values can be explained by the fact that, at large m, two edge flames are located far from the tip of the plate in both cases, and the interaction between them is small. It can also be seen that in both cases the blow-off values are determined

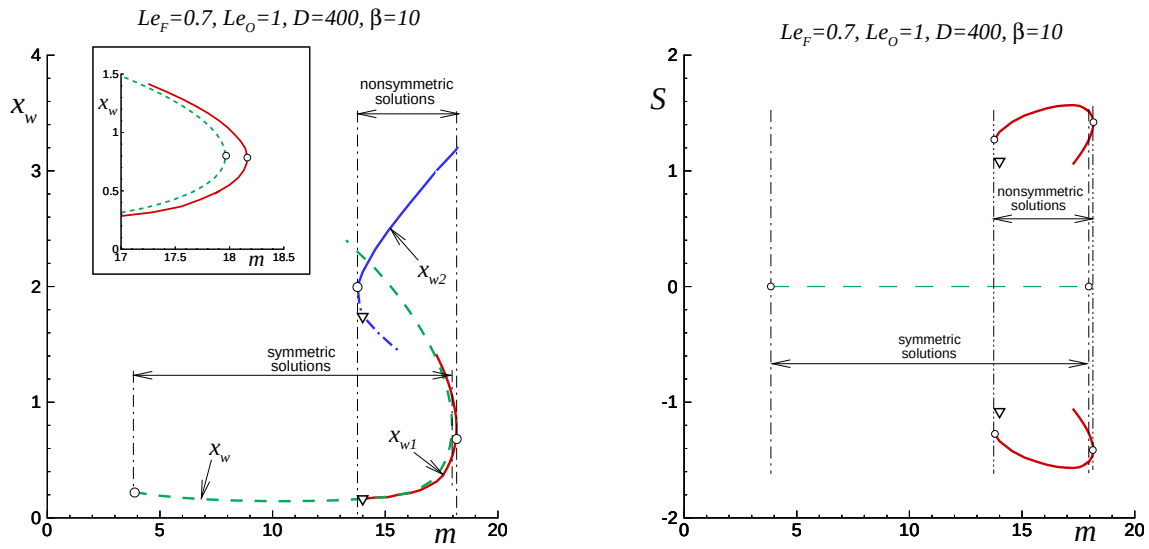

Figure 13: Dependencies of the x-coordinate (left plot) and symmetry index (right plot) for the edge-flame on the dimensionless gas velocity. The dashed line corresponds to symmetrical flames, the solid lines corresponds to the non-symmetrical flames. The open circles show the critical points for flame extinction and blow-off. Open triangles correspond to an intermediate (unstable) solution obtained by a time-dependent method.

by the turning point, as illustrated in the inset on the left plot. As usual, the states corresponding to the parts of the curves above the turning point are unstable.

In all likelihood, a turning point also limits the existence region for non-symmetrical flames near m_{min}, which does not happen for symmetric flames. It is interesting to note in Fig. 6 that for cases calculated with $y_p = -0.699$ and $y_p = -0.7$ the flame dynamics approaches an almost time-independent state (between $t \approx 10 \div 20$), which then nevertheless transitions, at larger times, to a symmetric or non-symmetric state. It can be conjectured that this intermediate state represents another non-symmetric steady state, which, however, is unstable (at large times). The corresponding point is marked in Fig. 13 by open triangles. Unfortunately, attempts to calculate this unstable branch completely were not possible due to the rigidity of the calculations, and the expected probable curve (indicated by a dash-dotted line) is continued manually in Fig. 13 (left).

The above results suggest that there are no bifurcation points that connect the symmetric and non-symmetric branches, that is, an island of non-symmetric solutions exists independently of the symmetric branch. The absence of bifurcation points is also indicated by the fact that for

each value of the flow rate m at which a non-symmetric flame exists, the symmetrical counterpart exists also and it is stable. This situation differs from what happens for flame propagation in channels [22–24] where symmetric and non-symmetric solutions also appear for the same value of the flow rate. In the latter case, bifurcation points between the symmetric and non-symmetric branches certainly exist, and when a non-symmetric solution appears, the corresponding symmetric solution becomes unstable.

5 Concluding remarks

If a system has different stable states, then it can be qualitatively concluded that even if all these states are stable to small perturbations, some of them are more stable than others if the perturbations imposed on the system are not small. Apparently, such a situation is possible in the case of a diffusion flame formed by the injection of parallel jets of fuel and oxidizer at the same speed. It is obvious that, upon successful ignition, combustion consists in two edge flames (in the planar case) localized immediately after the tips of the plates separating the streams and followed by diffusion flame tails. These two edge flame localizations are mirrored with respect to the symmetry line as shown in Fig. 5 (right plot). This is the expected symmetrical combustion pattern for this burner configuration.

However, it turns out that when the fuel Lewis number is less than one, the locations of the edge flames may be not symmetrical, as shown in Fig. 5 (left plot) and this state of the system is also stable. One can easily imagine a perturbation of this state (for example, when a short-acting heat source of sufficient intensity is applied), after which the combustion process will acquire a symmetrical structure (as shown in the sequence of Fig. 11). Nevertheless, it is difficult to imagine that some perturbation can transform a symmetric steady-state structure to a non-symmetric one. However, the non-symmetrical state is stable.

The numerical simulations presented in this paper show that in order to obtain a non-symmetric combustion pattern, the Zel'dovich number must be higher than a certain critical value. For the considered cases, this value turns out to be between 8.5 and 9. Numerical calculations also show the existence of critical values for the flow velocity and the reduced Damköhler number. To form a non-symmetric combustion pattern, the gas flow velocity must exceed and the Damköhler number must be less than the corresponding critical values.

The appearance of non-symmetric configurations can be clarified in the following qualitative way. When a localized hot spot is deposed only in one of the two cold mixing layers with

subsequent ignition, flame formation and consumption of fuel in this mixing layer together with a diffusion transversal flux of fuel towards the flame are established. This transfer increases for lower fuel Lewis numbers. With sufficient intensity of this transverse flux, the fuel mass fraction at the tip of the second plate becomes too small for the formation of another symmetrical edge flame. It should also be noted that an increase in the Zel'dovich number leads to a sharper dependence of the reaction rate on temperature, which also prevents the ignition of the adjacent mixing layer (in the case of non-symmetric ignition). However, it is obvious that a net increase in the Damköhler number contributes to the opposite effect, that is, ignition in the adjacent mixing layer becomes more likely. All these features promotes the formation of a non-symmetrical combustion pattern.

It should be noted that despite the introduced simplifying assumptions, the problem formulation contains a number of parameters whose influence on the flame structure has not been studied. Such parameters are, for example, the size of the hot spot used for ignition or the temperature distribution within it. The purpose of this study was not to compile a complete parametric-space map showing the zones in which non-symmetrical combustion patterns are formed. It seems that the construction of such a map is practically impossible. The main goal was to demonstrate that the emergence of stable non-symmetrical flame structures is possible in a situation of complete symmetry of the governing equations and boundary conditions with respect to the mirror transformation. The present results may be useful in the design of combustors with a split supply of fuel and oxidizer, especially for fuels with low Lewis number, such as hydrogen.

Acknowledgement

This work was financed by project #PID2019-108592RB-C42 / AEI / 10.13039/501100011033.

References

[1] G.R. Ruetsch, L. Vervisch, A. Liñán, Effects of heat release on triple flames, *Phys. Fluids A* 7 (1995) 1447-1454.

[2] J. Daou, A. Liñán, The role of unequal diffusivities in ignition and extinction fronts in strained mixing layers, *Combust. Theor. Model.* 2 (1998) 449477.

[3] S. Ghosal, L. Vervsich, Theoretical and numerical study of a symmetrical triple flame using the parabolic flame path approximation, *J. Fluid Mech.* 415 (2000) 227-260.

[4] R. Daou, J. Daou, J. Dold, Effect of heat-loss on flame-edges in a premixed counterflow, *Combust. Theor. Modell.* 7 (2003) 221242.

[5] R.W. Thatcher, A.A. Omon-Arancibia, Multiple speeds of flame edge propagation for Lewis numbers above one, *Combust. Theor. Model.* 9 (2005) 647-658.

[6] M.S. Cha, P.D. Ronney, Propagation rates of nonpremixed edge flames, *Combust. Flame* 146 (2006) 312-328.

[7] J. Daou, F. Al-Malki, Triple-flame propagation in a parallel flow: an analytical study, *Combust. Theor. Model.* 14 (2010) 177202.

[8] P. Pearce, J. Daou, The effect of gravity and thermal expansion on the propagation of a triple flame in a horizontal channel, *Combust. Flame* 160 (2013) 2800-2809.

[9] V.N. Kurdyumov, M. Matalon, Radiation losses as a driving mechanism for flame oscillations, *Proc. Combust. Int.* 29 (2002) 45-52.

[10] V.N. Kurdyumov, M. Matalon, Dynamics of an edge flame in a mixing layer, *Combust. Flame* 139 (2004) 329-339.

[11] V.N. Kurdyumov, M. Matalon, Stabilization and onset of oscillation of an edge-flame in the near-wake of a fuel injector, *Proc. Combust. Int.* 31 (2007) 909-917.

[12] V. Kurdyumov, M. Matalon, Effects of thermal expansion on the stabilization of an edge-flame in a mixing-layer model, *Proc. Combust. Int.* 32 (2009) 1107-1115.

[13] J.A. Bieri, M. Matalon, Edge flames stabilized in a non-premixed microcombustor, *Combust. Theor. Model.* 15 (2011) 911-932.

[14] J.A. Bieri, V.N. Kurdyumov, M. Matalon, The effect of gas expansion on edge flames stabilized in narrow channels, *Proc. Combust. Int.* 33 (2011) 1227-1234.

[15] K.-P. Liao, M. Matalon, C. Pantano, A flow pattern that sustains an edge flame in a straining mixing layer with finite thermal expansion, *Proc. Combust. Inst.* 35 (2015) 1015-1021.

[16] Z. Lu, M. Matalon, Edge flames in mixing layers: Effects of heat recirculation through thermally active splitter plates, *Combust. Flame* 217 (2020) 262-273

[17] B. Shields, J.B. Freund, C. Pantano, Stationary edge flames in a wedge with hydrodynamic variable-density interaction, *Combust. Flame* 211 (2020) 347-361.

[18] V.N. Kurdyumov, M. Matalon, Dynamics of an edge-flame in the corner region of two mutually perpendicular streams, *Proc. Combust. Int.* 31 (2007) 929-938.

[19] J.Buckmaster, Edge-flames, *Prog. Eng. Combust. Sci.* 28 (2002) 435-475.

[20] S.H. Chung, Stabilization, propagation and instability of tribrachial triple flames, *Proc. Combust. Inst.* 31 (2007) 877-892.

[21] A. Liñán, M. Vera, A.L. Sanchez, Ignition, liftoff, and extinction of gaseous diffusion flames, *Annu. Rev. Fluid Mech.* 47 (2015) 293-314.

[22] V.N. Kurdyumov, Lewis number effect on the propagation of premixed flames in narrow adiabatic channels: Symmetric and non-symmetric flames and their linear stability analysis, *Combust. Flame* 158 (2011) 1307–1317.

[23] V.N. Kurdyumov, C, Jiménez, Structure and stability of premixed flames propagating in narrow channels of circular cross-section: Non-axisymmetric, pulsating and rotating flames, *Combust. Flame* 167 (2016) 149–163.

[24] C. Jiménez, V.N. Kurdyumov, Propagation of symmetric and non-symmetric lean hydrogen-air flames in narrow channels: Influence of heat losses, *Proc. Combust. Int.* 36 (2017) 1559-1567.